NOTES AND CORRESPONDENCE

Lidar Observation of the Cirrus Cloud in the Tropopause at Chung-Li (25°N, 121°E)

J. B. NEE, C. N. LEN, W. N. CHEN, AND C. I. LIN

Department of Physics and Chemistry, National Central University, Chung-Li, Taiwan

14 May 1996 and 5 November 1997

ABSTRACT

The authors have detected a cirrus cloud near the tropopause by using a lidar system located at Chung-Li, Taiwan (25°N, 121°E). The cloud usually appeared between the month of May and September. In 1993–95, the cloud was observed almost 50% of the time that the lidar operated.

The cloud was detected in the heights between 15 and 17 km; the region of the atmosphere had a temperature ranging between −70° and −83°C. It was never detected above the tropopause. The cloud was characterized by its very thin structure. The geometrical and optical thicknesses are about 0.6 km and 0.008, respectively, which can be considered as a subvisual cloud. This paper reports more than 20 cloud events observed in the years between 1993 and 1995. Some properties of the clouds are listed and compared with other references.

1. Introduction

Clouds in the upper troposphere and lower stratosphere have attracted great attention recently because of their potential effects on the atmospheric radiation, climate, and chemistry. For example, polar stratospheric clouds (McCormick et al. 1982) have been extensively investigated for their roles in destroying the Antarctic ozone. However, information about the high clouds found outside the polar regions is very rare.

Properties of the high clouds in the atmosphere have been reported in several papers (Dowling and Radke 1990; Sassen and Cho 1992; Liou 1986; Platt et al. 1987; Woodbury and McCormick 1983; McFarquhar and Heymsfield 1996). Most of the clouds listed in the papers were found at about 70%–80% of the height of the tropopause, with temperatures ranging between −40° and −55°C; however, a few cirrus clouds reported were detected near the tropopause in the equatorial regions (Heymsfield 1986; Takahashi and Kuhara 1993; Knollenberg et al. 1993; Heymsfield and McFarquhar 1996).

High clouds in the tropopause were described in several studies. An important event reported by Heymsfield (1986) was about the observation of a cloud in the tropical region at an altitude of 16 km. The cloud was sampled and analyzed. The results indicated ice particles of trigonal plate and column type with sizes of typically 50 μm. Particle sizes of the tropical cirrus clouds located near the tropopause were recently investigated and reported in a few experiments (Takahashi and Kuhara 1993; Knollenberg et al. 1993; Heymsfield and McFarquhar 1996). The results of these measurements all indicated high concentrations of small ice particles, with low ice water content. The cloud heights, extensive horizontal coverage, and geographic locations from these observations are similar to what we have observed. This kind of cloud should be easily detected by lidar if it has properties as reported. The lack of such observational data may be due to limited observation facilities in this region.

The presence of the tropical tropopause cloud may be detectable by satellites. The occurrence of high clouds as measured by the Stratospheric Aerosol and Gas Experiment (SAGE) II in low latitudes has been recently discussed by Wang et al. (1994). The SAGE II satellite has the capability of observing high cloud with small optical thickness under subvisual conditions. However, SAGE II results revealed a particle size distribution (with mode radius 0.6 μm) much smaller than the sizes measured by in situ experiments (Heymsfield 1986; Takahashi and Kuhara 1993; Knollenberg et al. 1993; Heymsfield and McFarquhar 1996).

We have recently set up a lidar system to observe high clouds and aerosols existing in the upper troposphere and stratosphere. It interested us very much when we detected the tropopause cloud at the very beginning of the operation of our lidar. Later, we found the tropopause cloud appeared frequently in the summer months in 1993–95. The purpose of this paper is to report the preliminary results of the lidar measurements.

The temperature of the upper troposphere and lower

Corresponding author address: Dr. J. B. Nee, Department of Physics, National Central University, Chung-Li, Taiwan 32054.
E-mail: jbnee@phyast.phy.ncu.edu.tw

TABLE 1. Seasonal average of the temperature and height of the tropopause from June 1993 to May 1994.

Season	Summer (Jun 1993–Aug 1993)	Fall (Sep 1993–Nov 1993)	Winter (Dec 1993–Feb 1994)	Spring (Mar 1994–May 1994)
Temperature (C°)	−78.1	−79.0	−79.8	−79.2
Height (km)	16.9	17.0	17.3	17.3

stratosphere is critical to understanding the existence of the clouds. We have analyzed radiosonde data in 1990–95 provided by the Central Weather Bureau to support the cloud research. These data provide useful information about temperature and height of the local tropopause, as well as wind in these regions.

2. Instrumentation

The NCU lidar system was established in 1993 on the campus of the National Central University (NCU) at Chung-Li (25°N, 121°E), Taiwan. It consists of a YAG laser at 532 nm (Spectra Physics model GCR-4-30) operating at 30 Hz. The laser beam is steered into the vertical direction by a motor-controlled mirror mounted on an optical bench. The receiver consists of a 17.5-in. Newtonian-type telescope. A photomultiplier tube with a narrowband interference filter (FWHM 3 nm) was employed as the detector. The photon counting signals were sent to a multichannel analyzer (MCA, Stanford Instrument SR430) for signal analysis. The results were then sent to a PC486 for storage and further treatment.

The lidar system always operates on nights with good weather conditions. Measurements were carried out with laser energy 30–100 mJ (about 10 ns pulse width). Because we employed a photon-counting mode in the detection of the signals, the cloud could be seen with just 15 mJ of laser energy or about 0.5 W of power. In general, signals scattered from the low-level haze are much stronger than signals from the upper atmosphere. To avoid this problem, our system is optically aligned to heights greater than 10 km so that low-level clouds and aerosols would not interfere with the observation.

The range bin width was set at a resolution of 24 m per channel. Usually 9000 laser shots, which correspond to 5 min in real time, were summed to generate one data profile recorded in the MCA memory to be sent to the computer. Three MCA profiles (corresponding to 27 000 laser shots) were further averaged to produce a cloud profile shown in this paper. Data were treated by comparing the scattering signals of the clouds relative to clear air. The derived backscattering ratio is defined as

$$r = \frac{\beta_{\text{air}} + \beta_c}{\beta_{\text{air}}},$$

where β_{air} and β_c are, respectively, the backscattering

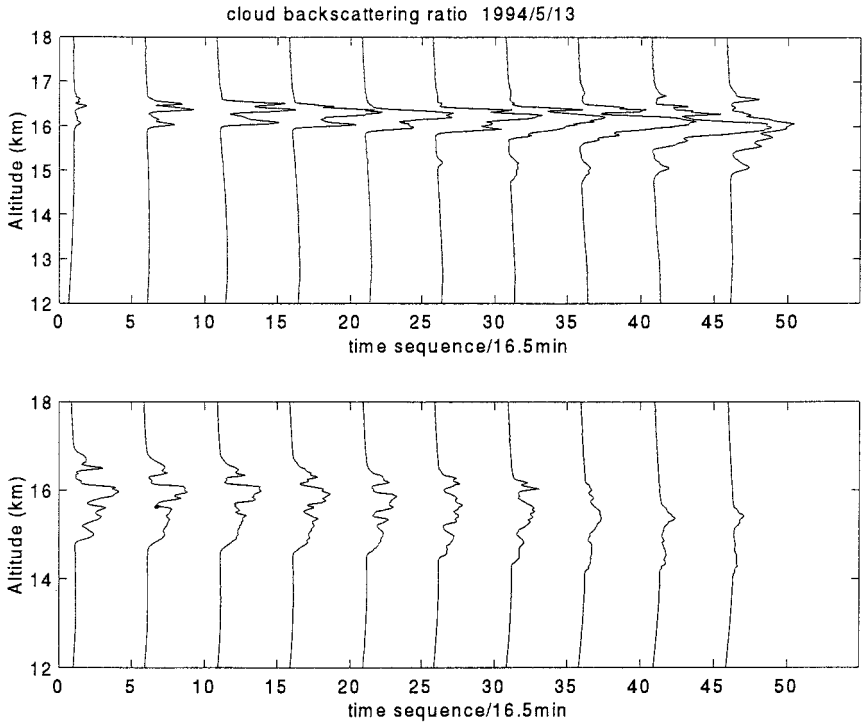

FIG. 1. Time sequence for cirrus cloud detected on 13 May 1994. The cloud profiles are expressed in two columns where the lower column is continued from the upper column. The cloud started at 2320 LST and disappeared toward daybreak. Each profile resulted from integration of data for 16.5 min and was plotted with the backscattering ratio progressively offset by 5.

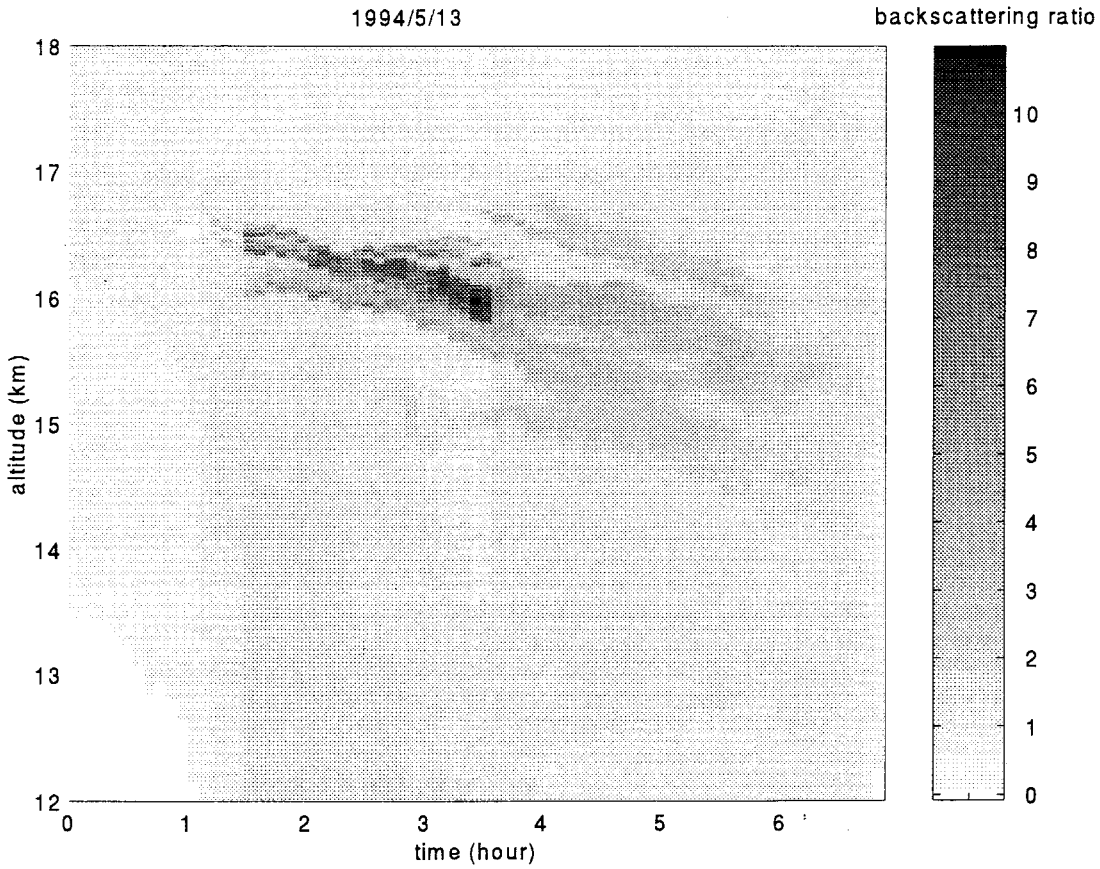

FIG. 2. A continuous scan of 13 May cloud shown in Fig. 1.

coefficient of air and cloud particles (Fernald et al. 1972; Reagan et al. 1989). To calculate the optical thickness, an empirical constant, S_A, defined as the ratio of the extinction to the backscattering coefficient is needed (Fernald et al. 1972; Reagan et al. 1989), which is proportional to the optical thickness. The value of S_A was adjusted in the calculations. In our calculations, we employed a constant value $S_A = 30$, which is close to the range of values used by many authors (Fernald et al. 1972; Sassen and Cho 1989; Imasu and Iwasaka 1992).

The radiosondes (Vaisala module) from the Central Weather Bureau, providing data on temperature, dewpoint, and wind speed, were launched daily at 0800 and 2000 LST (0000 and 1200 UTC) at a station about 50 km north of the lidar site. The measurements are carried out at a time and place different from our lidar research; however, they provide a useful reference about the atmosphere.

We define the tropopause in this paper as the region where the lowest temperature is found. By this defini-

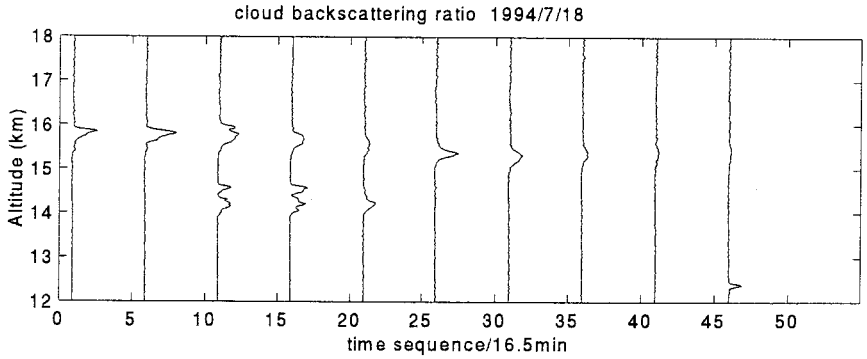

FIG. 3. Cloud observation in the evening of 18 July 1994. A cloud in the tropopause and a cloud in the upper troposphere were simultaneously observed.

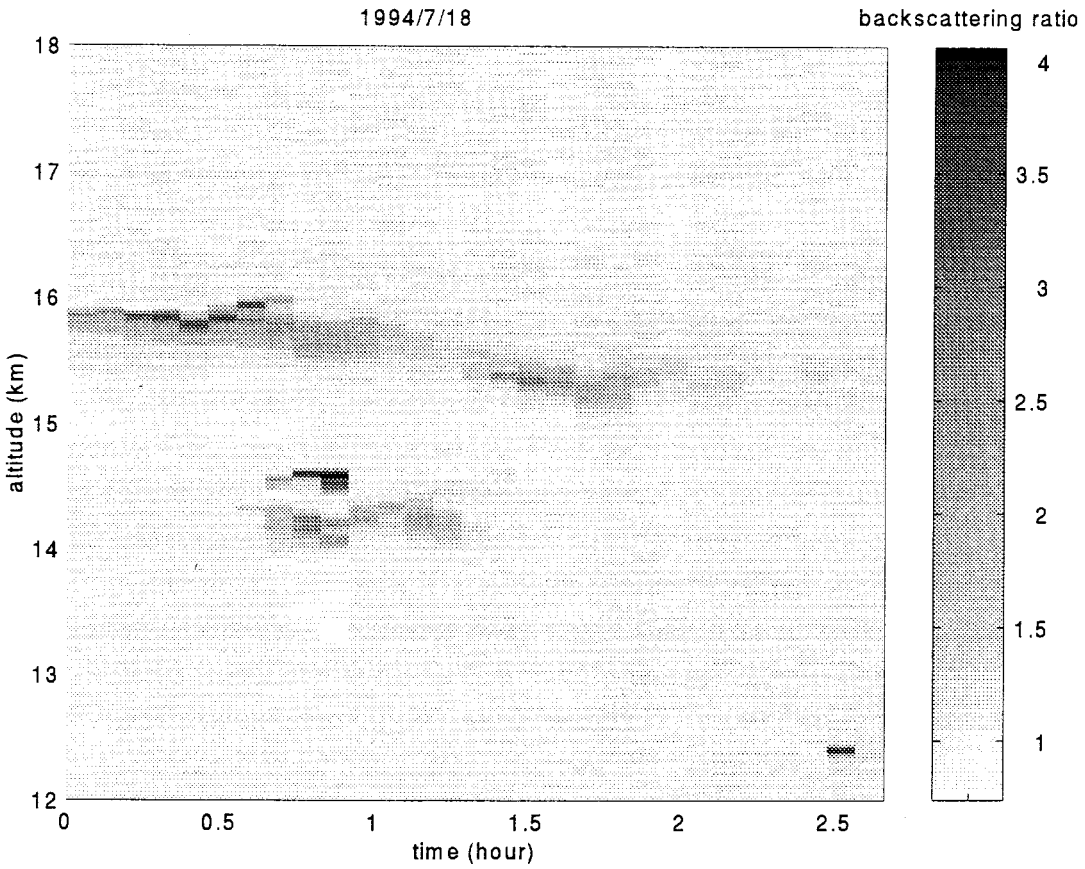

FIG. 4. A continuous scan of the cloud system observed on 18 July 1994.

tion, the average tropopause height in 1990–95 was 16.95 km with a temperature of −79.03°C. (The average tropopause height in 1994 was 17.02 km with a temperature of −79.26°C as shown below.) The meteorological tropopause, defined by $\Delta T/\Delta z \leq 0.2$°C for 2 km continuously, is located at about 15 km throughout the seasons. The seasonally averaged temperature and height of the tropopause are shown in Table 1. The humidity at the tropopause is very important for the understanding the formation of the tropopause cloud. However, it has been recognized that the humidity measurements by radiosonde are not accurate enough at low temperature conditions (Pratt 1985). For this reason, the humidity data were not used.

3. Results

A typical and complete observation of the tropopause cloud is shown in Fig. 1. The cloud was detected in the evening on 13 May 1994. A continuous scan of the cloud is shown in Fig. 2. The cloud appeared at 2320 LST and developed into full strength in about 15 min. Initially, the cloud was found at 16 km and was quite narrow with a thickness of approximately 600 m as shown in the upper column of Fig. 1. More specifically as shown in the fourth profile, the major peak was located at 16.3 km. It steadily descended to a height of 16 km in the 10th profile. A descending speed of 180 m h^{-1} (5 cm s^{-1}) can be determined using these data. Several hours later, the cloud diffused to a thickness of 2 km and became weakened starting from 0400 LST toward daybreak as shown in the last three profiles in Fig. 1. Each profile in Fig. 1 resulted from integration of data for about 16.5 min (or about 27 000 laser shots). Figure 2 shows more clearly the evolution of the cloud in grayscale.

Temperature measurement of the radiosonde revealed that the lowest temperature in the night of 13 May was −80.5°C at a height of 18.9 km (70 mb) where the wind speed was 5.6 m s^{-1}.

Figure 3 shows another such cloud observed on 18 July 1995. The cloud was first detected near 16 km, which was about 1 km below the low temperature point defined in this paper as the tropopause. Later, a separate cloud was detected at about 14 km as shown in Fig. 3. The lower cloud at 14 km was less persistent and did not seem to correlate with the tropopause cloud. The tropopause cloud often lasted through the whole night. Figure 4 is the continuous scan of the cloud.

In the years of 1993 and 1994, more than 20 events

TABLE 2. Properties of cirrus clouds observed and related meteorology data.

Date (da/mo/yr)[i]	Time[a]	Height (km)[b]	T(C)[c]	Thick (km)[d]	τ[e]	Wind θ[f]	Wind v (m s^{-1})[g]	Remarks[h]
1 Sep 1993	0100	15.43	−74.6	0.456	0.0052	162	11.3	
13 May 1994	2200	16.25	−70.4	0.552	0.0207	26.8	3.1	
27 Jun 1994	2200	16.20	−78.8	0.48	0.0041	74	18.3	
28 Jun 1994	2200	16.44	−80.4	0.672	0.0045	69	20.2	
29 Jun 1994	0225	15.79	−74.7	1.25	0.0093	59.3	18.5	
30 Jun 1994	2315	15.98	−78.8	1.77	0.036	88	24.5	
1 Jul 1994	0125	13.5–16.1	−68.9	2.95	0.142	107	21.9	14.74
18 Jul 1994	2120	15.81	−77.1	0.334	0.0029	125.3	6.0	
19 Jul 1994	2130	15.92	−77.5	0.24	0.0016	140	7.3	
20 Jul 1994	0010	12.6–15.0	−61.5	1.19	0.094	270	9.4	13.84 km
1 Aug 1994	2210	13–15.80	−71.8	2.30	0.0255	85.2	28.8	15.7 km
3 Aug 1994	0115	15.24	−71.9	0.288	0.0016	115	7.8	
18 Aug 1994	2356	15.53	−71.3	0.168	0.0008	76.8	9.6	
19 Aug 1994	0243	15.62	−71.8	0.31	0.0042	125	4.6	
11 Sep 1994	0005	16.42	−76.1	1.08	0.0053	73.8	8.4	
27 Sep 1994	0018	16.34	−78.8	0.192	0.0008	172	6.6	
28 Sep 1994	1245	17.21	−83.1	0.127	0.0033	128	8.5	
4 Sep 1995	2137	13.9–17.1	−71.0	1.80	0.112	87	18.2	15.41 km
5 Sep 1995	0046	12.5–16.5	−72.7	1.97	0.027	57.5	16.6	15.86 km
7 Sep 1995	2226	13.5–15.3	−74.8	1.724	0.0336	89.6	22.6	16.25 km
11 Sep 1995	2342	16.78	−78.2	1.08	0.0217	108	8.4	

[a] Time (LST) for first appearance of the cloud, or the lidar start time if a cloud already existed.
[b] Height for maximum backscattering ratio.
[c] Temperature from radiosonde.
[d] Thickness for a well defined profile.
[e] Optical thickness.
[f] Wind direction (θ) in degrees.
[g] Wind speed v.
[h] Multilayer clouds, height for the layer of maximum backscattering ratio R.
[i] Tropopause clouds were also observed on 16 Jul, 1 Sep, 4 Aug, 7 Aug, 31 Aug, 26 Sep, 9 Dec 1993, but data were not adequate for analysis.

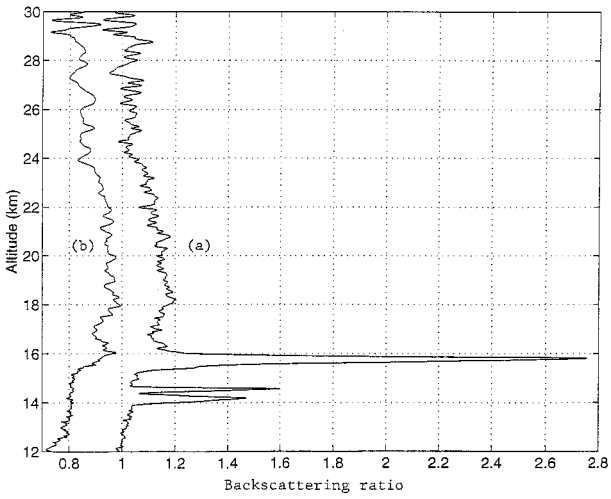

FIG. 5. (a) The overlapping of a cirrus cloud with the stratospheric aerosol. The cloud was detected at 2200 LST 19 July 1994. (b) The cloud disappeared 2 h (2400 LST) later but an enhanced layer of aerosol was left. Both profiles resulted from an average of 10 measurements.

of high clouds were detected out of about 40 observation nights. Thus, the chance of observing high clouds was about 50% during the summer in these years. In 1995 we did not operate the lidar for the entire summer due to a breakdown of the laser system in June and July. However, detection of the cloud was still frequent in August and September. The clouds occurred usually from early summer in May to fall in October. The tropopause is coldest in January and February based on the radiosonde data; however, we have not detected such cloud in these months so far (up to writing of this paper in 1996). This lack of observation may be partially due to poor weather conditions in the winter so that we have less chance to operate our lidar (we may set the probability to be less than 10%).

Table 2 lists about 20 high clouds observed in 1993–96 with date, time, height, temperature, thickness (km), optical thickness, wind direction, and wind speed given. We mainly list clouds observed above 15 km, but some multilayer clouds covering a few thousand meters are also included since they extended to the tropopause. Since the cloud profile varied during the observation, the strongest profile in the early stage in each observation was analyzed to give its height, temperature, thickness, and optical thickness. The thickness is defined here to be the full width of the half maximum of the

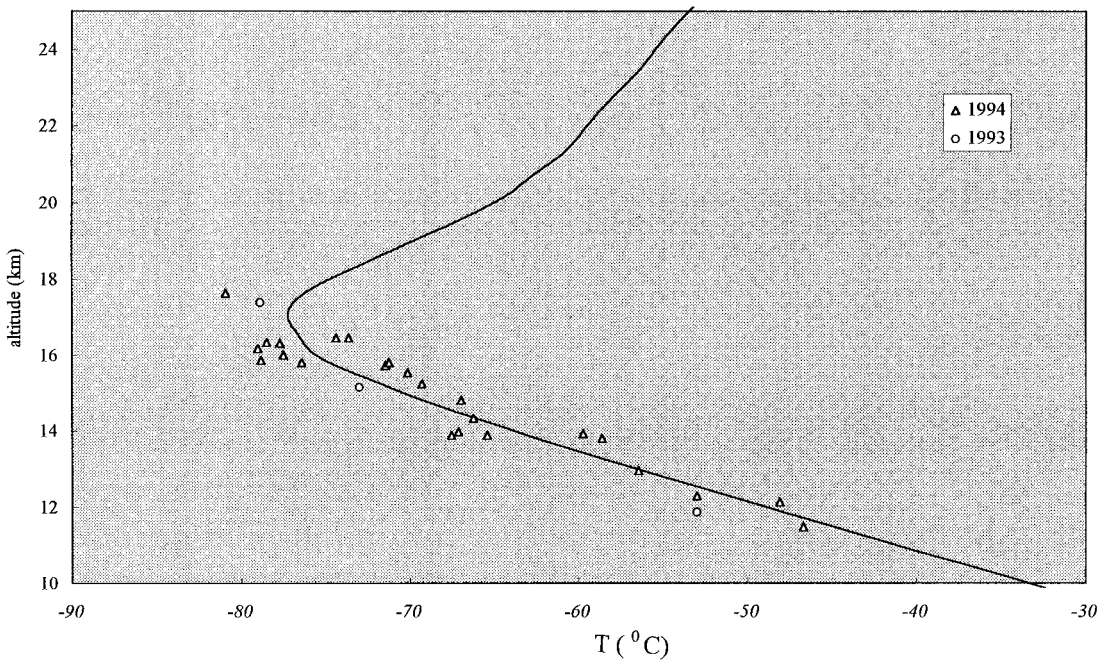

FIG. 6. Heights and temperatures of the tropopause clouds detected in 1993 and 1994. The solid line is the annual average of the atmospheric temperature measured by the radiosonde.

largest profile. Using the data in Table 2, we may calculate some averaged properties about the cloud. Excluding the multilayer clouds, our tropopause cloud has an average temperature of −76.2°C, thickness 0.6 km, and optical thickness 0.008. The temperature and wind data were taken from radiosonde records.

The tropopause cloud can be generally classified as subvisual. The mean optical thickness 0.008 is smaller than the threshold value 0.03 defined by Sassen and Cho (1992) for invisible cirrus cloud. Seeing the cloud with the naked eye was impossible since one can still see the faint stars in the sky. Thus, although the sky is overcast, it looks clear.

There must be a strong correlation between the high cloud and stratospheric aerosols, since they overlap very much in the same heights. Figure 5 shows both the tropopause cloud and aerosols. In Fig. 5a, a tropopause cloud was detected as usual, with the background aerosol plotted. The cloud later disappeared and left in the aerosol an enhanced layer as shown in Fig. 5b.

4. Discussion

a. Cloud climatology

Climatology conditions near Taiwan based on the meteorological satellite were reported by Ferraro et al. (1996) and Stowe et al. (1989). Based on microwave sounding SSM/I, Ferraro et al. showed the maps of global rainfall, clouds, and water content. In the summer months (June, July, and August), the global rainfall and rainfall frequency are highest in the equatorial region of the Pacific. Taiwan is located just outside the rim of the highest rainfall region, which is characterized by the relatively high total precipitable water and high integrated cloud liquid water, but relatively lower cloud frequencies compared with equatorial regions.

Stowe et al. (1989) investigated the global cloud climatology based on *Nimbus-7* data in 1979 and compared with previous reports. Although Stowe et al. presented data for the weather of January and July only, we may take the July data as representative of the summer months. Their results showed a high total cloud amount but low total cloud day in the region around Taiwan in July. This is equivalent to low cloud frequency, which is consistent with Ferraro et al. (1996). The cloud data are further characterized by a low amount of low clouds (heights of 0–2 km), higher amount of middle clouds (2–7 km), and highest amount of high clouds (≥7 km). *Nimbus-7* data showed the occurrence of high density of cirrus cloud in regions of west Pacific near the Tropics, with the maximum frequency of occurrence in the region of southeast Asia and the Bay of Bengal. This high cirrus cloud region shifts to the Southern Hemisphere in northern Australia in January. The map of the deep convection is similar. Taiwan is on the edge of this high density of cirrus cloud. Thus *Nimbus-7* data may be very useful in understanding the occurrence of high cirrus cloud in the equatorial regions.

Table 2 lists data about the wind conditions related to the observation of the cloud. For example, wind direction indicates that east wind (90°) is dominant in the summer. (Further information is found in the appendix

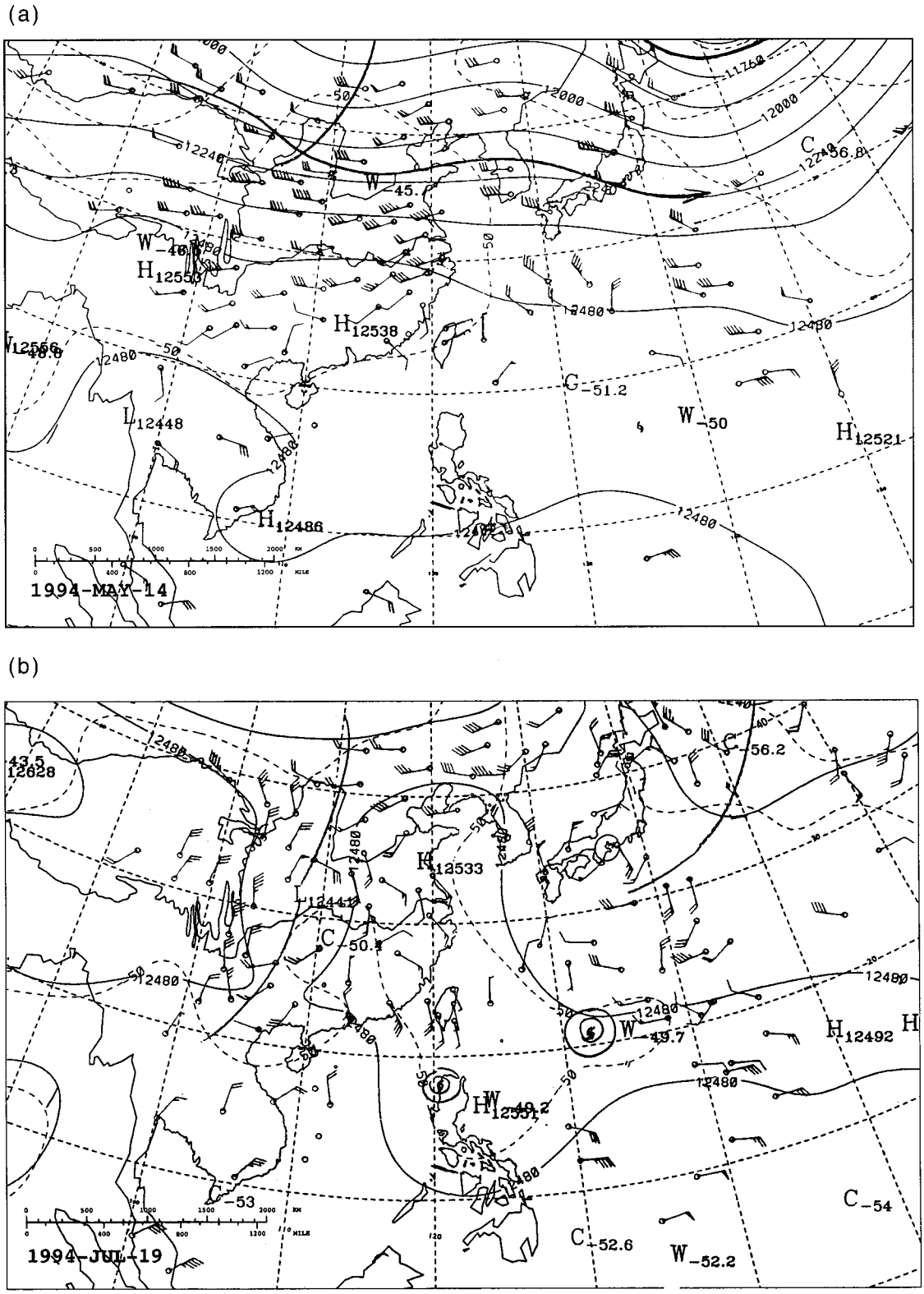

FIG. 7. (a) Upper-air map at 200 hPa, 0800 LST 14 May (0000 UTC) 1994. (b) Upper-air map at 200 hPa, 0800 LST 19 July (0000 UTC) 1994.

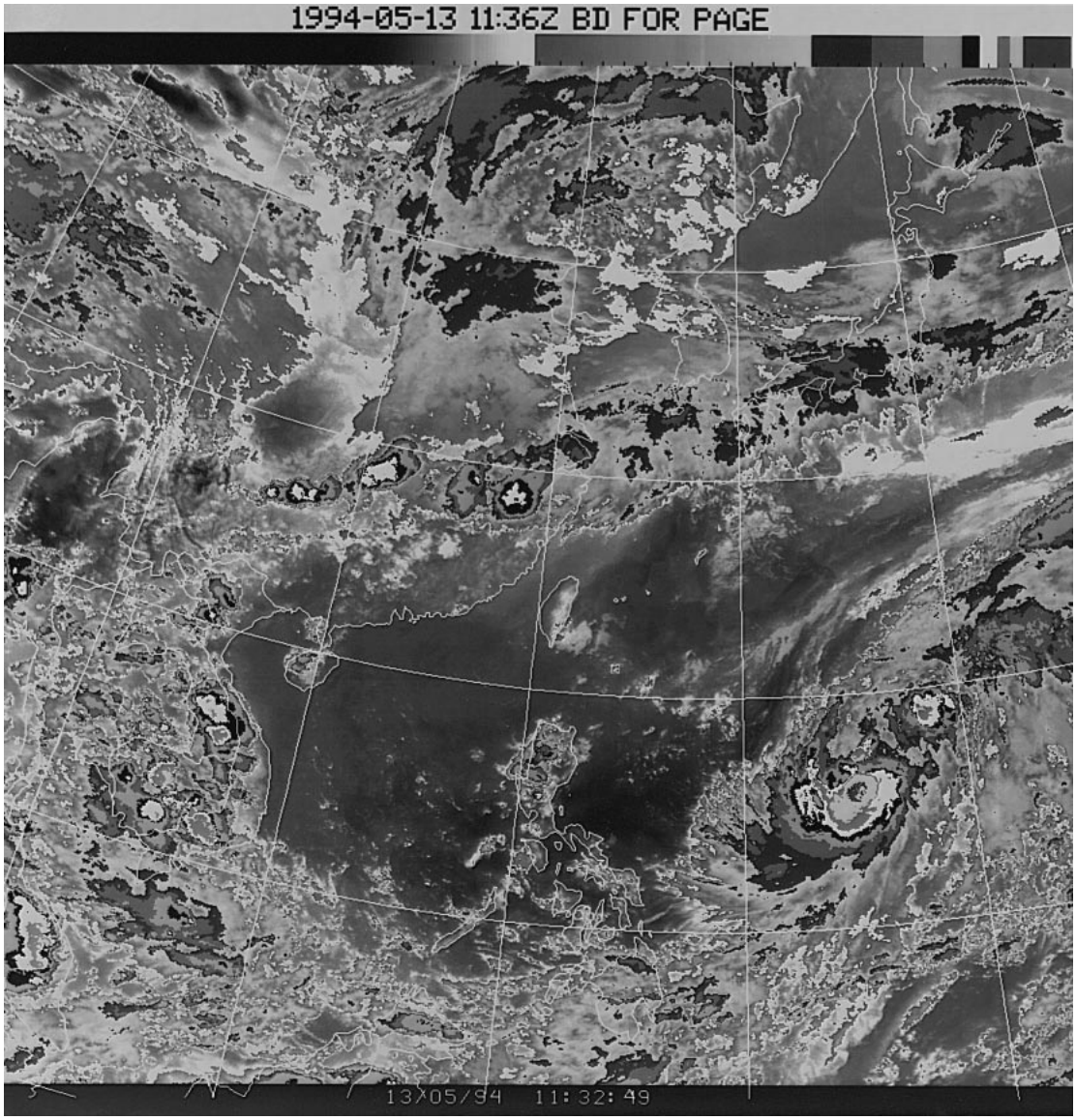

FIG. 8. GMS infrared satellite picture on 13 May 1994.

for cases when cirrus clouds were detected, including 200-hPa maps and *GMS-4* IR map).

b. Cloud properties

Some properties of the tropopause cloud may be inferred from our observations. The cloud is usually located below the tropopause by less than 1 km but occasionally approached the tropopause. The highest cloud we detected was slightly above 17 km (on 29 September 1994). However, the tropopause on this day was at 17.5 km (−83.7°C). The heights and temperatures of the clouds observed in 1993 and 1994 are plotted in Fig. 6. The temperature profile in Fig. 6 is the average of the atmospheric temperature measurements at 100-m intervals during 1990–95 obtained from the radiosonde data.

The horizontal spread of the cloud must be large enough to be regularly detected by lidar. This is because the laser beam expands to a diameter of 10 m at a height of 15 km, and the detection of clouds is by no means accidental. In addition, there is wind in the tropopause as recorded by the radiosonde. For example, the wind speed at the tropopause for 13 May 1994 was 5.6 m s^{-1} (3.8 m s^{-1} at the cloud). Since the cloud lasted for at least 6 h, its horizontal size must be larger than 100 km. This is consistent with previous observation of Heymsfield (1986), who found that the tropopause cloud had a horizontal extent larger than 350 km (Heymsfield 1986). Such clouds may be also detected by SAGE II, as reported by Wang et al. (1994). However, SAGE II results showed smaller cloud occurrence in summer than in winter. Our frequent detection of the cloud in the

summertime may be related with our geological location.

The rate of descent for a stable cloud may reveal its particle sizes. The descent rate of various type of ice particles has been investigated by Heymsfield (1972). By assuming that the ice particles are either plates or columns, we found that the ice particle size could be either a plate with a diameter of 25 μm or a column with a length of 15 μm using formulas in Heymsfield's paper. This is consistent with the particle size distribution of the tropopause clouds measured by in situ experiments (Heymsfield 1986; Takahashi and Kuhara 1993; Knollenberg et al. 1993; Heymsfield and Mc-Farquhar 1996) but larger than the particle sized given by SAGE II.

The tropopause cloud as we defined it in this paper is so far not well understood. It has been described in a few papers (Heymsfield 1986; Takahashi and Kuhara 1993; Knollenberg et al. 1993; Heymsfield and Mc-Farquhar 1996), but its properties are not known since such data are still rare. We are currently measuring the microphysical properties about these clouds using the depolarization ratio and multiwavelength detection. Since tropical tropopause is where air is ''freeze-dried'' before entering into the stratosphere, the cloud at the tropical tropopause may be very important for the understanding of the global circulation of air and dehydration process in the stratosphere (Kley et al. 1982; Newell and Gould-Stewart 1981).

5. Conclusions

This paper presents results of ground-based lidar observations of high clouds near the tropopause. More than 20 events of cloud data are listed, including their height distribution, temperature, thickness, and wind conditions. The cloud has a thin structure, both geometrically and optically, and is located at a height where the average temperature is about -76°C. This cloud can be classified as a subvisual cloud. In 1993–95, we observed the cloud 50% of the time we operated the lidar. Its location within the aerosol layer may indicate that they are closely related.

Acknowledgments. This research is supported by the National Science Council of the ROC under Contract NSC85-2112-M008-012.

APPENDIX

Analyses at 200 hPa and *GMS-4* Satellite Weather Picture

Figures 7a and 7b, respectively, show the upper-air maps for 200 hPa at 0000 LST 14 May (0000 UTC) 1994 and 0000 LST 19 July 1994. Data supplied by Center Weather Bureau, Taiwan. Figure 8 shows a satellite picture taken by GMS infrared channel on 13 May 1994. The cloud picture shows haze over the Taiwan area, but it might be caused by the low clouds. Since low-level cloud and haze are often dominant, the satellite cloud picture is not very useful for this purpose. Furthermore, since the tropopause cloud is subvisual, it is not known if the cloud is detectable by the weather satellite.

REFERENCES

Dowling, D. R., and L. F. Radke, 1990: A summary of physical properties of cirrus clouds. *J. Appl. Meteor.,* **29,** 970–978.

Fernald, F. G., B. M. Herman, and J. A. Reagan, 1972: Determination of aerosol height distribution by lidar. *J. Appl. Meteor.,* **11,** 482.

Ferraro, R. F., F. Weng, N. C. Grody, and A. Basist, 1996: An eight year (1987–1994) time series of rainfall, clouds, water vapor, snow cover, and sea ice derived from SSM/I measurements. *Bull. Amer. Meteor. Soc.,* **77,** 891–905.

Heymsfield, A. J., 1972: Ice crystal terminal velocities, *J. Atmos. Sci.,* **29,** 1348–1357.

——, 1986: Ice particles observed in a cirriform cloud at -83°C and implications for polar stratospheric clouds. *J. Atmos. Sci.,* **43,** 851–855.

——, and R. M. Sabin, 1989: Cirrus crystal nucleation by homogeneous freezing of solution droplets. *J. Atmos. Sci.,* **46,** 2252–2264.

——, and G. M. McFarquhar, 1996: High albedos of cirrus in the tropical pacific warm pool: Microphysical interpretations from CEPEX and from Kwajalein, Marshall Islands. *J. Atmos. Sci.,* **53,** 2424–2451.

Imasu, R., and Y. Iwasaka, 1992: A new analytical procedure to derive the scattering parameter of optically thin clouds from lidar data. *J. Geomag. Geoelectr.,* **44,** 277–287.

Kley, D., A. L. Schmeltkopf, K. Kelly, R. H. Winkler, T. L. Thompson, and M. McFarland, 1982: Transport of water vapor through the tropical tropopause. *Geophys. Res. Lett.,* **9,** 617–620.

Knollenberg, R. G., K. Kelly, and J. C. Wilson, 1993: Measurements of high number densities of ice crystals in the tops of tropical cumulonimbus. *J. Geophys. Res.,* **98,** 8639–8664.

Liou, K., 1986: Influence of cirrus clouds on weather and climate processes: A global perspective. *Mon. Wea. Rev.,* **114,** 1167–1199.

McCormick, M. P., H. M. Steele, P. Hamill, W. P. Chu, and T. J. Swissler, 1982: Polar stratospheric cloud sightings by SAM II. *J. Atmos. Sci.,* **39,** 1387–1397.

McFarquhar, G. M., and A. J. Heymsfield, 1996: Microphysical characteristics of three anvils sampled during the Central Equatorial Pacific Experiment. *J. Atmos. Sci.,* **53,** 2401–2423.

Newell, R. E., and S. Gould-Stewart, 1981: A stratospheric fountain? *J. Atmos. Sci.,* **38,** 2789–2795.

Platt, C. M. R., J. C. Scott, and A. C. Dilley, 1987: Remote sounding of high clouds. Part VI: Optical properties of midlatitude and tropical cirrus. *J. Atmos. Sci.,* **44,** 729–747.

Pratt, R. W., 1985: Review of radiosonde humidity and temperature errors. *J. Atmos. Oceanic Technol.,* **2,** 404–407.

Reagan, J. A., M. P. McCormick, and J. D. Spinhirne, 1989: Lidar sensing of aerosols and clouds in the troposphere and stratosphere. *Proc. IEEE,* **77,** 433–448.

Sassen, K., and B. S. Cho, 1992: Subvisual-thin cirrus lidar dataset for satellite verification and climatological research. *J. Appl. Meteor.,* **31,** 1275–1285.

Stowe, L. L., H. Y. M. Yeh, T. F. Eck, C. G. Wellemeyer, H. L. Kyle, and the Nimbus-7 Cloud Data Processing Team, 1989: Nimbus-7 Global cloud climatology. Part II: First year results, *J. Climate,* **2,** 671–708.

Takahashi, T., and K. Kuhara, 1993: Precipitation mechanisms of cumulonimbus clouds at Pohnpei, Micronesia. *J. Meteor. Soc. Japan,* **71,** 21–31.

Wang, P. H., M. P. McCormick, L. R. Poole, W. P. Chu, G. K. Yue, G. S. Kent, and K. M. Skeens, 1994: Tropical high cloud characteristics derived from SAGE II extinction measurements. *Atmos. Res.,* **34,** 53–83.

Woodbury, G. E., and M. P. McCormick, 1983: Global distributions of cirrus clouds determined from SAGE data, *Geophys. Res. Lett.,* **10,** 1180–1193.